Hexagonal Microbolometer Pixel for Flexible Substrates

Çiğdem Yıldızak and M. Yusuf Tanrıkulu

Adana Science and Technology University, Adana, Turkey
cyildizak@adanabtu.edu.tr, mytanrikulu@adanabtu.edu.tr

Abstract

Nature becomes a source of inspiration to many researches on imaging systems. Imaging features owned by biological forms such as high resolution, wide field of view, high depth of field, high sensitivity to motion and light are attractive reasons to mimic the nature in imaging system applications. In this study, an arthropod eye's hexagonal shaped ommatidia are taken as a model for uncooled microbolometer pixel structure. A hexagonal pixel with 34 μm diagonal length which has the thermal conductance value of 1.48×10^{-7} W/K and the time constant value of 0.69 ms is designed for the first time in literature. The pixels are estimated to have an NETD of less than 250 mK in a potential 384x288 microbolometer array.

1. Introduction

High resolution and wide field of view are desired features of imaging systems. In many imaging applications, it is inspired from nature to obtain an imaging system that has wide field of view and high resolution. Insects have compound eye structure constructed by tiny eye arrays each called as ommatidium that consists of the lens, receptors, and associated structures [1]. Ommatidia are typically in hexagonal shape in the top view. Fig. 1 shows a hemispherical arthropod eye and its zoomed version to see the hexagonal shaped ommatidia. The array of ommatidia is settled in a hemispherical structure. This settlement provides ability of sight in a wide angle to the arthropods. This feature becomes an inspiration for many imaging applications [2-4]. Not only the arthropod eyes but also other curved eye structured animals becomes a model to many imaging system researches [5-7].
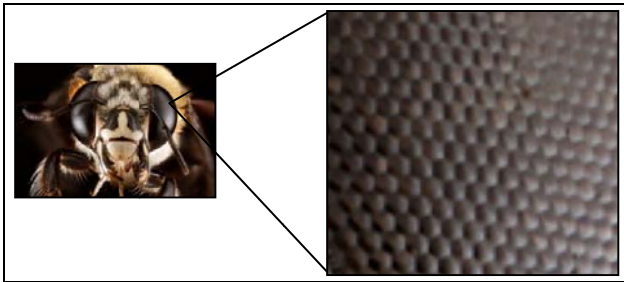

Fig. 1. Arthropod eye and its zoomed hexagonal ommatidia [8].

Like other imaging systems, increasing the field of view and resolution are important design considerations for infrared imaging. Operating at room temperature without any cooling requirement, ability to be fabricated monolithically on CMOS readout circuits, having low cost, low weight and low power dissipation, and beside these advantages, operating on a large spectral range make uncooled microbolometers used in many areas like thermography, automotive, surveillance, and military. Typical uncooled microbolometers consist of planar substrate with planar detector pixels on it. The structure of substrate and the shape of the pixels can affect the yield of the microbolometer [9]. A microbolometer with curved substrate can provide a panoramic view, and therefore increase the field of view compared to microbolometer with planar substrate.

In this study, it is aimed to design a hexagonal microbolometer pixel suitable for a curved substrate imitating a bug eye to obtain increased field of view. Fig. 2 shows these detectors on a spherical substrate. Although there are studies to fabricate bolometers on flexible substrates [10-12], hexagonal microbolometers for these substrates are proposed for the first time in literature.
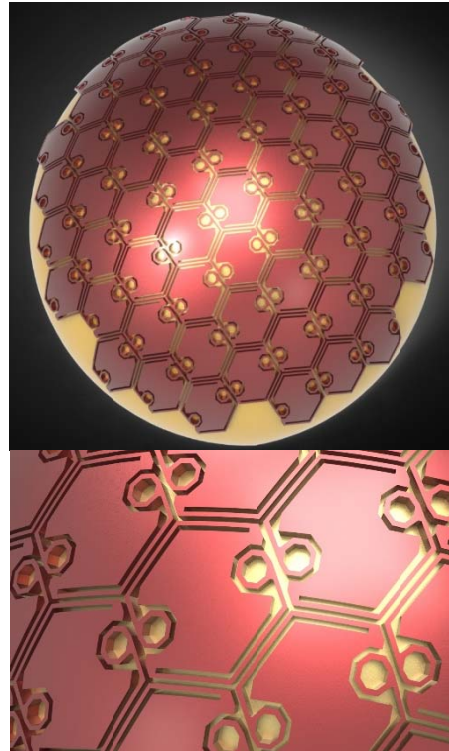

Fig. 2. Designed hexagonal microbolometer detectors on a spherical substrate and its zoomed version.

2. Physical and Performance Parameters of Microbolometers

There are various physical parameters affecting the performance of microbolometers. The most important ones are thermal conductance, thermal capacitance, and thermal time constant.

The thermal conductance is the parameter showing the isolation level of the pixel from the substrate. It directly depends on the physical dimensions and the thermal conductivities of the layers in the support arms. The thermal conductance can be found as:

$$G_{th} = \frac{2\sigma A}{L} \qquad (1)$$

where σ is thermal conductivity of the material used in the support arm, A is the cross-sectional area of the support arm, and L is the length of the support arm.

Thermal capacitance is the parameter that shows how much heat can be stored. It is expressed as:

$$C_{th} = V\rho C_p \qquad (2)$$

where V is the volume of the active detector area, ρ is the density, and C_p is the heat capacity of the material.

The thermal time constant expresses how fast the detector gives response to infrared radiation. It is desired to have smaller thermal time constant value to obtain faster detectors. The thermal time constant is specified by:

$$\tau = \frac{C_{th}}{G_{th}} \qquad (3)$$

where C_{th} is the thermal capacitance and G_{th} is the thermal conductance.

These parameters affect directly the responsivity and noise equivalent temperature difference (NETD) of the pixels which are the most important performance parameters. Responsivity is the electrical response of the detector with respect to absorbed unit infrared power and it is expressed as:

$$\Re_v = \frac{\eta I_d R_d \alpha}{G_{th}} \qquad (4)$$

where η is the absorption coefficient, I_d is the detector current, R_d is the detector resistance, α is the temperature coefficient of resistance (TCR) value, and G_{th} is the thermal conductance. NETD is a performance parameter that shows how small temperature difference the microbolometer can detect the target scene. Smaller NETD indicates better performance. The NETD value is calculated by:

$$NETD = \frac{4F^2 V_n}{\tau_0 A_D \Re_v (\Delta P/\Delta T)_{\lambda_1 - \lambda_2}} \qquad (5)$$

where F is a function of distance from the optics to the target, V_n is the total RMS noise voltage, τ_0 is the transmission of the optics, A_D is the active detector area, $\Re_v$ is the voltage responsivity of the detector, $(\Delta P/\Delta T)_{\lambda_1-\lambda_2}$ is the change of power per unit area radiated by a blackbody at temperature T, measured within the spectral band of $\lambda_1-\lambda_2$.

The physical parameters are designed to get the maximum performance from the detectors, i.e., to maximize the responsivity and to minimize the NETD.

3. Design of Hexagonal Pixel

Fig. 3 shows the layout view of the designed hexagonal pixel for this study which has 34 μm diagonal distance together with the structural parameters. 34 μm is chosen to make a comparison with rectangular type pixel with a pitch of 35 μm. Arm and gap widths are selected as 1 μm due to fabrication requirements needed for a future fabrication process. ZnO is used as structural and absorber layers, and gold is used as mirror layer of the designed hexagonal pixel. The thickness of the ZnO is selected as 50 nm since the ZnO is planned to be coated with Atomic Layer Deposition (ALD) technique which is suitable for low thickness values.

Fig. 4 shows the 3-D view of the hexagonal microbolometer obtained using the COMSOL software and the process flow proposed in [13]. In the 3-D view, yellow area represents the mirror layer used to increase the absorption, and the red area represents structural and absorber layer of the hexagonal microbolometer structure.
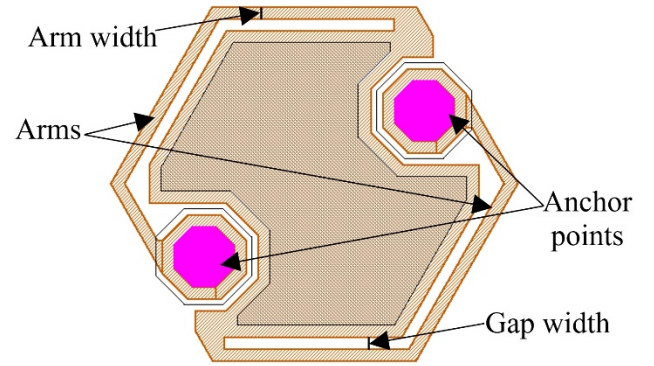

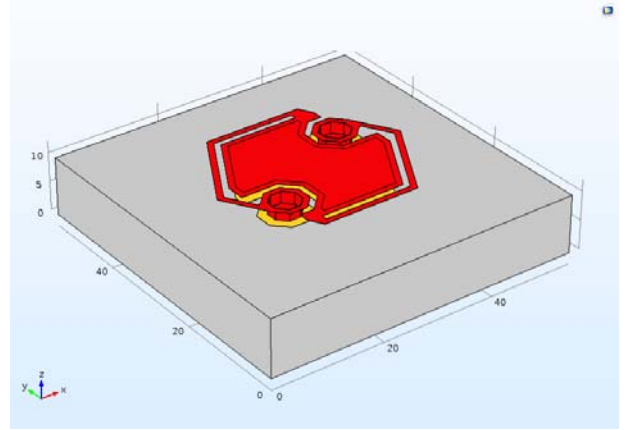**Fig. 3.** Hexagonal pixel layout and the structural parameters.

Fig. 4. 3-D view of the hexagonal pixel.

4. Thermal Simulations

After constructing the 3D model of the hexagonal microbolometer pixel, the thermal simulations are conducted using the COMSOL software. The physical parameters of ZnO required for the thermal simulations are taken from COMSOL database as: 5.67 gr/cm^3 for density, 505.73 J/kgK for heat capacity, and 61.85 W/mK for thermal conductivity . The simulations are realized by applying 100 nW heat to the pixel

for some time period and checking the steady-state temperature of the pixel together with the transient response. The heating curve is drawn according to the transient response which is actually the temperature value of the pixel corresponding to the fixed time steps.

Fig. 5 shows the thermal simulation results of both designed hexagonal pixel and a rectangular pixel that has 35 μm pixel pitch. The same structural parameters of 1 μm arm and gap widths with 50 nm ZnO thickness are used for the rectangular pixel to compare with the hexagonal pixel. It is observed that the steady-state temperature difference of the hexagonal pixel and the rectangular pixel are 0.676 K and 0.885 K, respectively. Thermal conductance (G_{th}) of the pixels are calculated with the applied heat divided by temperature difference, and obtained as 1.48×10^{-7} W/K for the hexagonal pixel and 1.13×10^{-7} W/K for the rectangular pixel. As can be seen from the results the hexagonal pixel having approximately same structural values with the rectangular pixel can provide close performance parameters.

Fig. 6 shows the heating curve of the hexagonal pixel. The thermal time constant of the hexagonal microbolometer pixel is obtained as 0.69 ms from the fitting result of the heating curve while it is 1.54 ms for the rectangular pixel. Both of the pixels are suitable for 30 fps infrared imaging which is the most common imaging speed [14]. The thermal time constant of the hexagonal pixel is lower making it suitable also for faster applications.
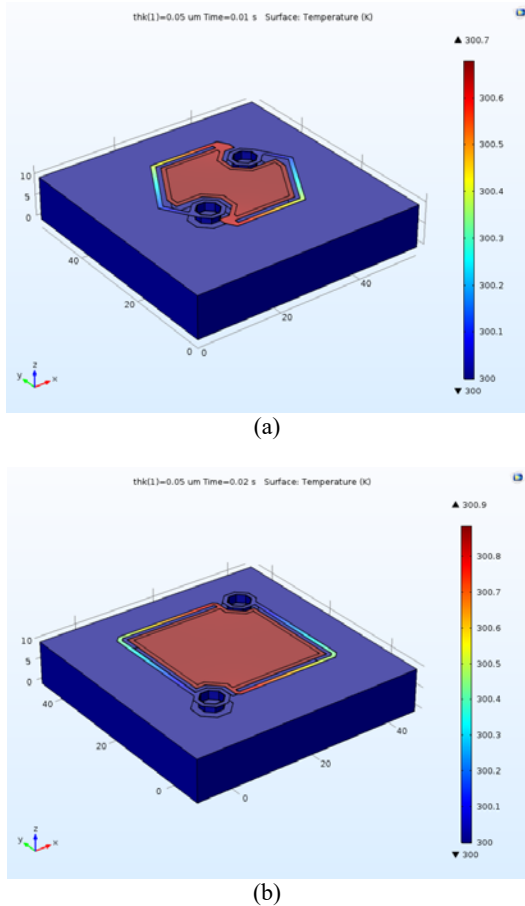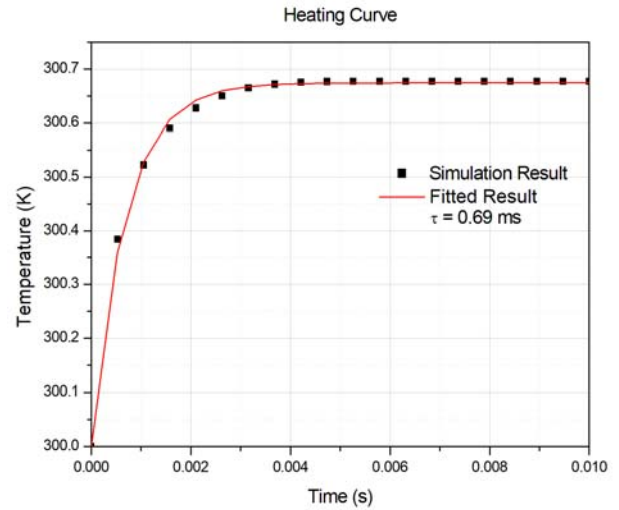

Fig. 6. Heating curve of the hexagonal pixel.

5. Conclusion

A hexagonal pixel based on inspiration of arthropod eyes is designed for flexible substrates for the first time in literature, and its thermal simulations are performed. The hexagonal pixel's structural parameters are chosen as 1 μm arm and gap widths, with 34 μm diagonal length. Gold is used as mirror layer and 50 nm thickness of ZnO is used as structural and absorber layer. According to thermal simulations realized by application of 100 nW heat, time constant is obtained as 0.69 ms and the thermal conductance is obtained as 1.48×10^{-7} W/K. Table 1 shows the physical parameters of the detectors together with some calculated performance values. When compared with the results of rectangular shaped microbolometer pixel, it is seen that the hexagonal shaped pixel has a good potential to be used in especially flexible infrared imaging systems in terms of its thermal features.

(a)

(b)

Fig. 5. Thermal simulation results of the (a) hexagonal pixel and (b) rectangular pixel.

Table 1. The physical parameters of the detectors together with some calculated performance values.

Parameter	Hexagonal Pixel	Rectangular Pixel
Pixel dimensions (μm)	34 (Diagonal)	35 x 35
Resistance (kΩ)	135	
Active detector area (μm²)	358.4	689.3
Fill factor (%)	47.5	56.3
TCR (%/K)	-10.4	
Thermal conductance (W/K)	1.48×10^{-7}	1.13×10^{-7}
DC responsivity (V/W)	6.98×10^{5}	9.2×10^{5}
Absorption coefficient (%)	50	
FPA size	384 x 288	
Integration time @30 fps	100	
Electrical bandwidth (kHz)	5	
Detector noise (μVrms)	27	
Transmission of optics	0.93	
NETD (mK)	221.5	87.4
Time constant (ms)	0.69	1.54

6. Acknowledgements

7. References

[1] M. F. Land, D. E. Nilsson, "Animal Eyes", Oxford University Press, 2nd Edition.

[2] U. K. Sur, "Bio-inspired hemispherical digital cameras of wide-angle field of view", Current Science, vol. 107, no. 1, 10 July 2014.

[3] Y. M. Song, Y. Xie, V. Malyarchuk, J. Xiao, I. Jung, K. J. Choi, Z. Liu, H. Park, C. Lu, R. H. Kim, R. Li, K. B. Crozier, Y. Huang, and J. A. Rogers, "Digital cameras with designs inspired by the arthropod eye", Nature, doi: 10.1038/nature12083, May 2013.

[4] D. Floreano, R. P. Camara, S. Viollet, F. Ruffier, A. Brückner, R. Leitel, W. Buss, M. Memouni, F. Expert, R. Juston, M. K. Dobrzynski, G. L'Eplattenier, F. Recktenwald, H. A. Mallot, and N. Franceschini, "Miniature curved artificial compound eyes", PNAS, vol. 110, no. 23, doi: 10.1073/pnas.1219068110, June 4, 2013.

[5] H. Liu, Y. Huang, and H. Jiang, "Artificial eye for scotopic vision with bioinspired all-optical photosensitivity enhancer", PNAS, vol. 113, no. 15, doi: 10.1073/pnas.1517953113, April 12, 2016.

[6] R. A. Street, W. S. Wong, and R. Lujan, "Curved electronic pixel arrays using a cut and bend approach", AIP, vol.105, no.10, doi: 10.1063/1.3129315, May 2009.

[7] B. Guenter, N. Joshi, R. Stoakley, A. Keefe, K. Geary, R. Freeman, J. Hundley, P. Patterson, D. Hammon, G. Herrera, E. Sherman, A. Nowak, R. Schubert, P. Brewer, L. Yang, R. Mott, and G. Mcknight, "Highly curved image sensors: a practical approach for improved optical performance", Optics Express, vol.25, no.12, doi: 10.1364/OE.25.013010, 30 May 2017.

[8] https://i.pinimg.com/originals/16/c7/4a/16c74a2c49955f12 0747ce7e683647bb.jpg, last accessed on 03.09.2017.

[9] A. W. Antesberger, "Alternative pixel shape for uncooled microbolometer", United States Patent, US 8,309,928 B2, Nov.13, 2012.

[10] A. Mahmood, S. Dayeh, D. P. Butler, Z. Çelik-Butler, "Micromachined Infrared Sensor Arrays on Flexible Polyimide Substrates", Sensors, 2003 IEEE, doi: 10.1109/ICSENS.2003.1279047.

[11] A. Yildiz, Z. Çelik-Butler, D. P. Butler, "Microbolometers on a Flexible Substrate for Infrared Detection", IEEE Sensors, vol.4, no.1, doi: 10.1109/JSEN.2003.820328, February 2004.

[12] A. Yaradanakul, D. P. Butler, Z. Çelik-Butler, "Uncooled Infrared Microbolometers on a Flexible Substrate", IEEE Transactions on Electron Devices, vol. 49, no. 5, doi: 10.1109/16.998605, May 2002.

[13] C. Yildizak, A. K. Okyay, M. Y. Tanrikulu, "Process Design and Thermal Simulations of a Single Layer Microbolometer", submitted to International Advanced Research And Engineering Congress (IAREC 2017), 2017.

[14] J. J. Yon, E. Mottina, and J. L. Tissot, "Latest amorphous silicon microbolometer developments at LETI-LIR," Proc. of SPIE, 2008. 6940. doi: 10.1117/12.780538.